Acoustic Communications and Navigation Under Arctic Ice

Lee Freitag, Peter Koski, Andrey Morozov, Sandipa Singh and James Partan
Woods Hole Oceanographic Institution
Woods Hole, MA USA
{lfreitag, pkoski, amorozov, ssingh, jpartan}@whoi.edu

***Abstract*— Initial results of experiments performed under Arctic ice have shown that acoustic communications and navigation can be performed on scales of 10-100 km using relatively inexpensive and compact hardware. Measurements of the impulse response at ranges of 10 and 75 km reveal extensive scatter and both resolvable and unresolvable rays. Phase coherent communication using adaptive equalization was successful up to ranges of 70-90 km at data rates of 5-10 b/s. As the SNR drops to levels too low for phase coherent communication, short FM sweeps (5-10 s), are shown to provide sufficient gain to provide lower rate communications and also support navigation.**

I. Introduction

Unmanned systems, whether powered, gliding or drifting, represent the best platforms for extensive sampling of the water under Arctic ice. However, navigation, telemetry and control of these platforms is made difficult because the ice makes it nearly impossible for them to surface safely. Thus, acoustics is the only practical long-range method for positioning and maintaining control of under-ice platforms [1]. However, while acoustic signals can propagate for long distances under ice, the signals scatter from the ice at each reflection, increasing loss and creating challenging propagation conditions for the receiver.

Here two range scales of current interest are addressed. One, on order 10 km, is suitable for short vehicle missions that focus on time scales less than 12-24 hours, for example using REMUS 100 class vehicles. The second range scale is intended to support gliders and floats on scales of weeks to months, and ideally over hundreds of kilometers, but at a minimum of 100 km. Data transmission at long ranges is challenging because of the high cost in energy for small vehicles, however, for future large vehicles, a modest amount of data could be sent to surface stations to provide position and mission status occasionally. An artist's rendition of the scenario, showing different classes of vehicles performing different missions, is presented in Figure 1.

The paper includes a description of the approach taken thus far, and initial results obtained during two recent experiments. The first experiment was performed in September 2010 in collaboration with the Nansen Centre in Norway aboard the icebreaker *K/V Svalbard*, and included ranges up to 100 km. The second, undertaken during a Navy test north of Alaska in March 2011, with environmental data from 2009 used for modeling, included ranges up to 75 km. In the latter case post-processing of the received signals showed that longer ranges could have been achieved at the lower end of data rates that were transmitted.

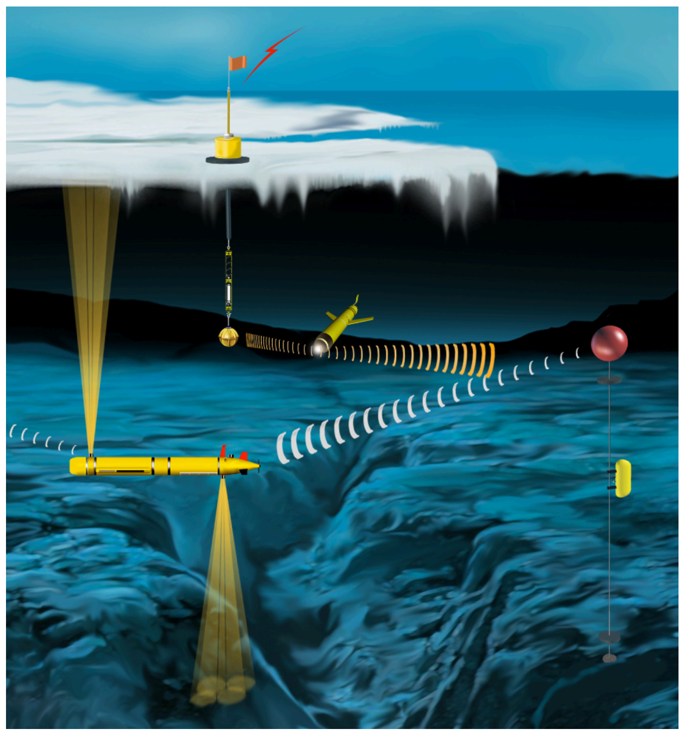

Figure 1. Gliders and powered AUVs performing oceanographic work beneath the Arctic ice.

A. Approach

Both navigation and communication can be accomplished using the same hardware components, and the challenge is to design transducers and processing to achieve the desired range, throughput and power efficiency. The acoustic source technology employed to achieve the long range while using a small, hand-deployed transducer is a simple Helmholtz resonator that consists of a spherical ceramic within a carefully designed but simple tube. A carrier frequency of approximately 700 Hz was used in one experiment, and 900 in the other. Bandwidths up to 96 Hz were explored, with 12 Hz being the most reliable at the maximum ranges. Additional background on the sources is presented in [2].

Two signaling approaches are considered: incoherent and coherent. The incoherent signals use FM sweeps that are matched-filtered and which may be used for both navigation and communication. The distance from a reference location is determined by the acoustic travel time of the signal, and very simple commands (a few bits) can be sent as well. Coherent signaling is more difficult and requires more bandwidth, but was shown during these two field trials to be effective as well. Low bit rates are still the norm, but 10s of bits per second at ranges of 40 km is possible, and a few bits per second at 90 km was also achieved. In this paper we focus on the phase-coherent results.

B. *Other Work*

There has been considerable research done in low-frequency acoustic propagation in the Arctic, both focused on acoustic anti-submarine warfare, and addressing the question as to whether acoustic tomography could be used to measure and monitor the temperature of the Arctic Ocean. Papers that explore the differences between open ocean and under-ice propagation include several that studied ice vs. non-ice covered propagation paths in the Greenland Sea [3-5]. Recent work in Norway by the Nansen Center and collaborating institutions has also explored tomography in the Fram Strait with the additional objective of navigating gliders under the ice [6].

The paper is organized as follows. In Section II the measured Alaska 2009 sound-speed profile is presented along with propagation modeling results and impulse response measurements for the short-range case. In Section III the results from the Fram Strait experiment are presented. Section IV describes the 2011 Alaska experiment and results. Conclusions and discussion of next steps are provided in the last section.

II. Modeling and Short-Range Propagation

The acoustic conditions are dominated by extensive reverberation caused by refraction that returns rays to the surface where they scatter off the underside of the ice. The refraction occurs not only deep where the pressure effect increases the sound speed, but at intermediate layers as well.

During the experiments described here CTD (during ICEX) and XBT (aboard the *K/V Svalbard*) measurements were made and used to estimate the propagation. The resulting sound speed profiles are specific to the dates and locations of these tests but provide realistic examples of recent conditions in the Arctic. The CTD profile taken from the ice camp in the Beaufort Sea in March 2009 shows a surface channel plus a deeper channel (Figure 2). The channel in 2011 contained similar features.

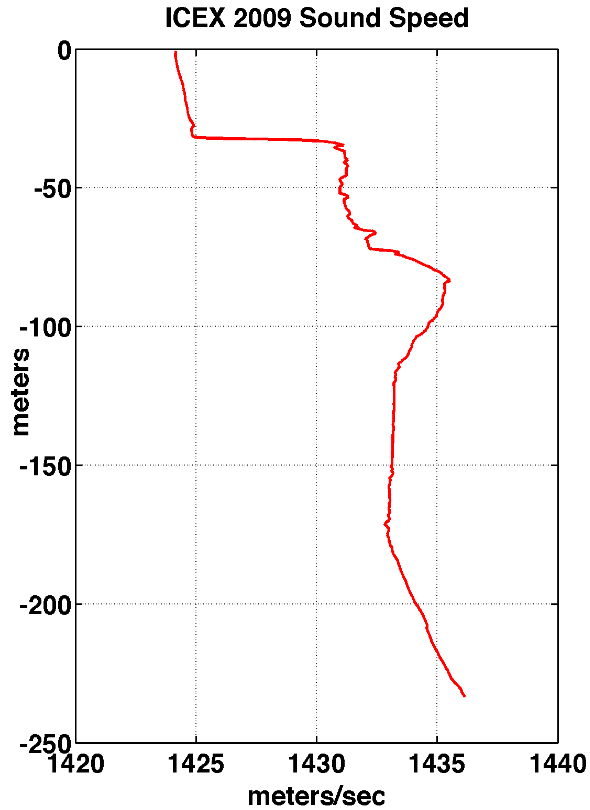

Figure 2. Sound speed showing the cold, low salinity surface layer followed by two possible sound channels.

Propagation loss for this profile shows surface-ducted propagation and two sets of rays that turn deeper, one at 75m which corresponds to the second step in the profile, the other at approximately 250 m where the sound speed again increases (Figure 3). This figure helps to illustrate the multipath complexity resulting from the sound speed structure: signals from a shallow source (the likely place for an under-ice profiling UUV) propagate in the surface duct, but also refract at the 75 m and 250 m positive sound speed gradients shown in Figure 2. The transmission loss for a source placed at 50 m (not shown) is significantly different; the direct path propagates at 50 m, while refracting rays that turn below intersect with the surface approximately every 1000 m while the deep-turning rays behave as shown in Figure 3, turning at 4 km and intersecting with the surface between 8 and 9 km.

The results of matched-filtering an FM sweep on four channels of a short array (2 m between hydrophones) to measure the channel impulse response is shown in Figure 4. The early arrivals (up to about 0.04 s), have a similar structure, and have traveled in the fast surface layer. The later arrivals, from 0.05 to 0.08 s show much less channel-to-channel coherence as the number of discrete arrivals grows and the bandwidth is insufficient to resolve them. However, the later, stronger, arrivals are likely the deep turning rays that are not scattered except from perhaps an initial bounce that creates the parallel path that intersects the surface near 9 km

(Figure 3).

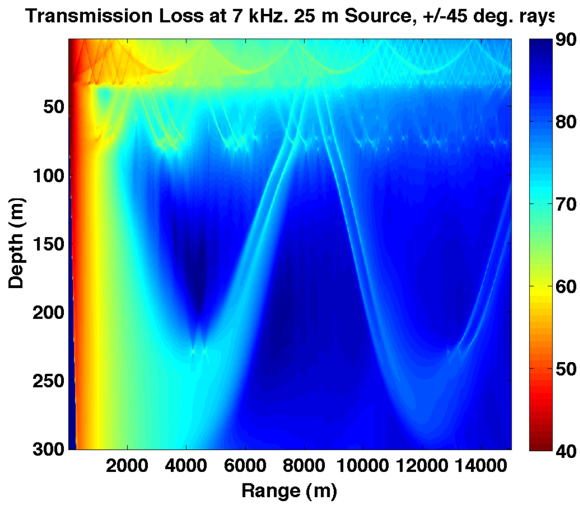

Figure 3. Transmission loss for a shallow source (25m).

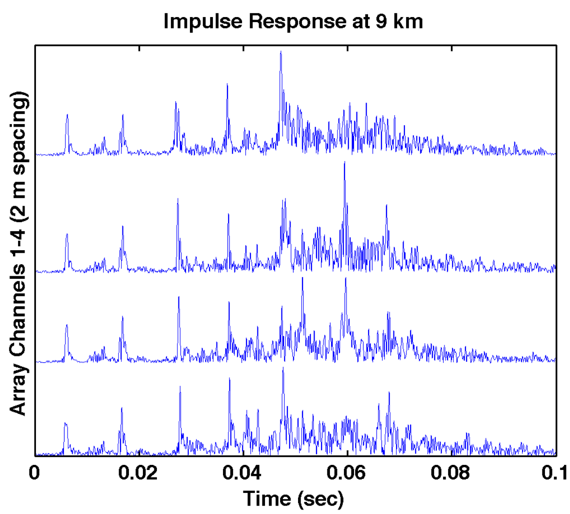

Figure 4. Measured impulse response at 7 kHz carrier with 4 kHz bandwidth FM sweep.

III. Experimental Results – Fram Strait

The Fram Strait experiment was done aboard the K/V Svalbard, on a joint expedition with the Nansen Center of Bergen, Norway in September 2010. The receiver, consisting of a small four channel array suspended 75 m below the ice was deployed at 79 26.3N, 000 19.5 W and the vessel then steamed directly to the west, stopping every 10 km to lower the 900 Hz acoustic source to 100 m for transmissions (Figure 5. The ice cover was approximately 80-90% as shown in Figure 6.

The propagation conditions included a cool, slow, surface layer extending to 150 m, thus the selected depths for source and receiver were within this layer. The profile for the area is shown in Figure 7. The propagation for this profile includes rays that turn away from the warmer, faster water below, and that either reflect from the surface, or refract at the shallow feature at approximately 20 m depth. The transmission loss clearly shows the trapped energy in the upper section of the water column, as well as the rays that turn at 500 m, the next sound speed maximum. During the transit to the west additional casts were made, showing the same basic features in the upper 150 m.


Figure 5 900 Hz Helmholtz resonator used for the Fram Strait experiment and deployed to 100 m at each station.


Figure 6 Ice conditions at the test area in the Fram Strait, Sept. 2010.

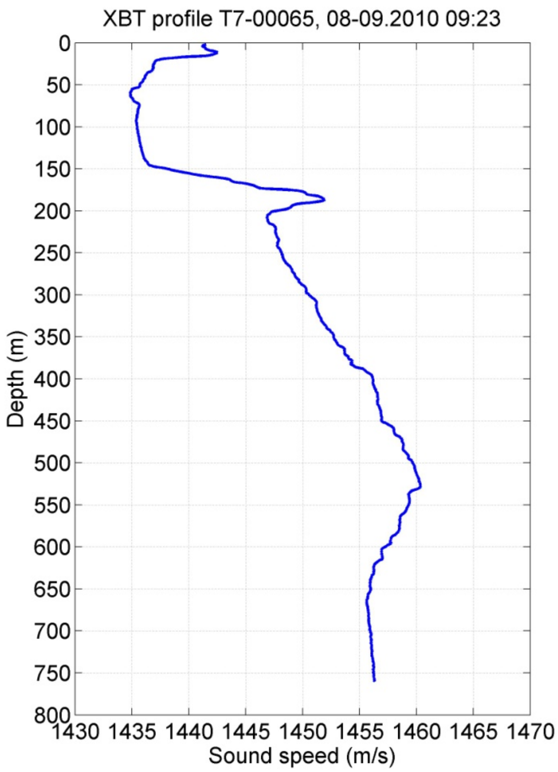

Figure 7 Fram Strait sound speed, Sept. 2010.

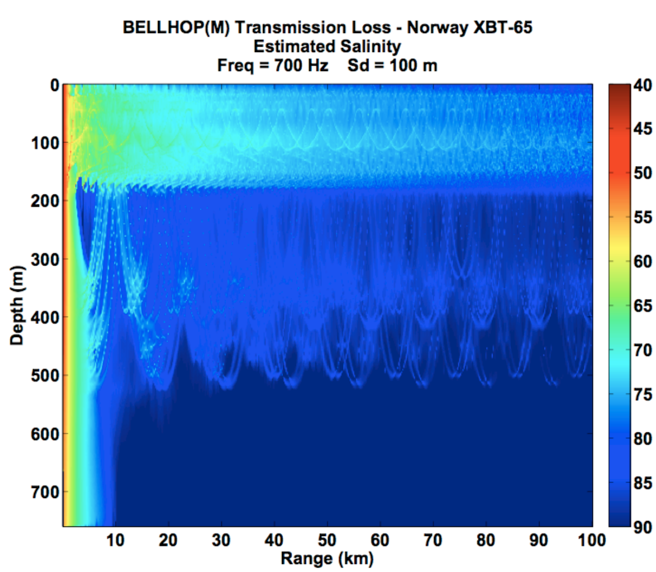

Figure 8 Transmission loss for the Fram Strait, Sept. 2010.

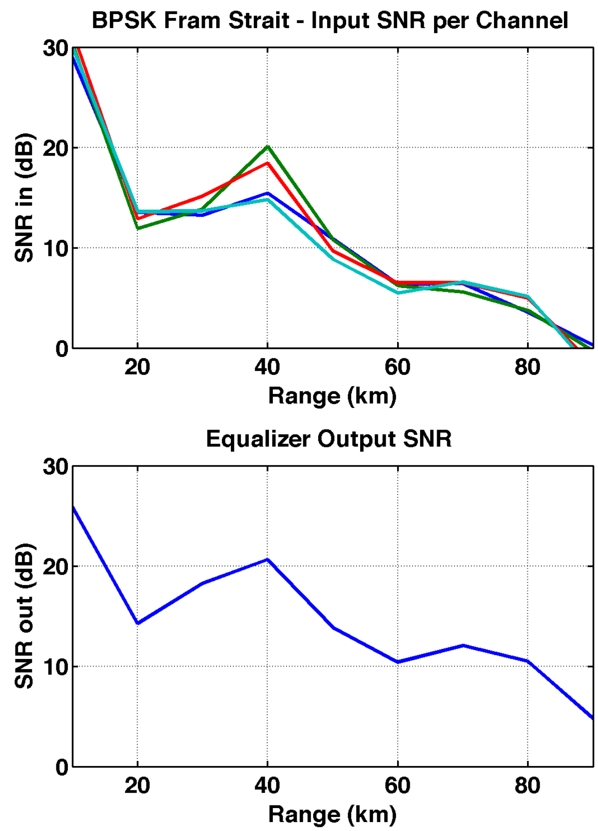

Figure 9 Fram Strait input and output SNR for a 12 Hz BPSK signal.

The results from the experiment can be characterized in terms of the input SNR to the receiver and the subsequent output SNR from the decision-feedback equalizer. The BPSK signal that was transmitted is examined with respect to its symbol rate (here focusing on the 12 Hz symbol rate data). As shown in Figure 9 the input SNR varies with range from 30 to near 0 dB, with a pattern that reflects the convergence of energy at 40 km and 70 km. The output SNR follows the same pattern, demonstrating (as expected) that signal level is an important determining factor for performance. The output SNR shows how at low SNR the multi-channel combining provides gain: the input SNR at 90 km is near zero, while the output is 5 dB.

Up to 80 km the output SNR of 10 dB or higher provides for symbol-rate communication, e.g. 12 bps. At 90 km the SNR is too low, and a high-rate code is required, reducing the data rate by approximately one-half.

Single-channel reception was also examined. An example is shown in Figure 10 where the receiver achieves 12 dB output SNR at 40 km, 8 dB less than the 4-channel solution.

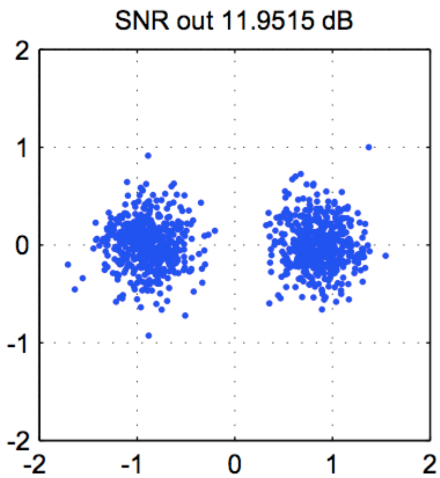

Figure 10 Single-channel equalizer result at 40 km

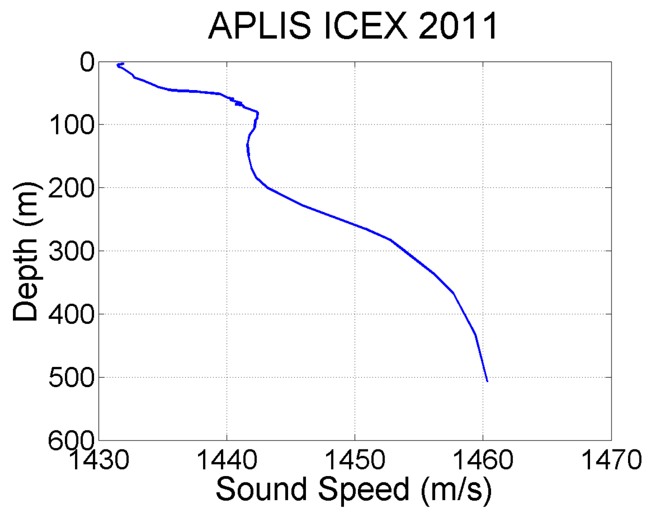

Figure 11 Sound speed computed from CTD data taken by Naval Postgraduate School officers in 2011.

IV. Experimental Results – ICEX 2011

In 2011 the Navy operated its biennial ICEX at the Applied Physics Laboratory Ice Station (APLIS), which is purpose-built to support the activity for two weeks in March. The camp hosts an underwater tracking range, acoustic communications (voice and data), and assists the submarines that are participating in the exercise to surface safely through the ice. In 2011 we were able to collect data using receivers deployed at 10, 20, 30 and 40 nmi from the camp, where a source was deployed through a hole melted in the ice under the control hut. While a number of experiments were performed using different sources, here the results of transmitting phase coherent signals at 700 Hz carrier are presented. The goal was to examine propagation from sources at different depths, and at multiple ranges. The ice coverage is high, greater than 90%, with leads opening and re-freezing regularly.

A. Sound Speed Profile and Propagation Conditions

The profile in 2011 was different than in 2009, the extremely well-defined surface layer of 2009 was instead a smoother transition to the bottom of the first layer. Also, there was no secondary layer at 75 m, though the channel at 150 m was present as before (see Figure 11 and compare with Figure 2).

Propagation from a shallow source is a primary focus of this work because ice-based transmitters are less expensive and easier to deploy when the required cables are very short. Given that the sound will propagate in any surface channel (if it exists), and also bend back to the surface, means that a shallow source is a viable option to transmit to platforms that are in the upper part of the water column.

Modeling was done using Bellhop with a perfectly absorbing bottom and perfectly reflecting surface in order to provide best-case results that illustrate the propagation patterns. Incorporating accurate surface loss is an important next step. In Figure 12 the ray pattern is shown for an 8 m source and it demonstrates the classic pattern of refracting rays that reflect from the surface at different ranges, depending on the initial angle.

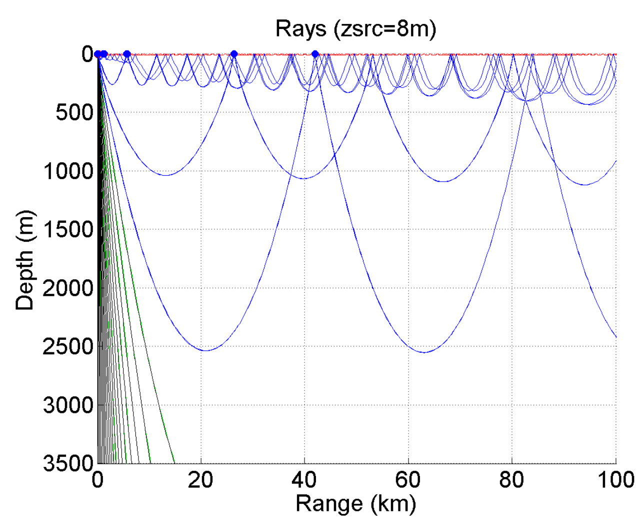

Figure 12 Simplified ray trace illustrating the surface propagation and two deeper sets of refracting rays.

The transmission loss, calculated without taking into account the scatter at the surface, shows the pattern of energy distribution with respect to depth and range (Figure 13). The effect of the channel at 150 m is clearly visible, with rays converging at the surface every 6-7 km. The figure also shows that energy will be present down to 1500 m without shadow zones.

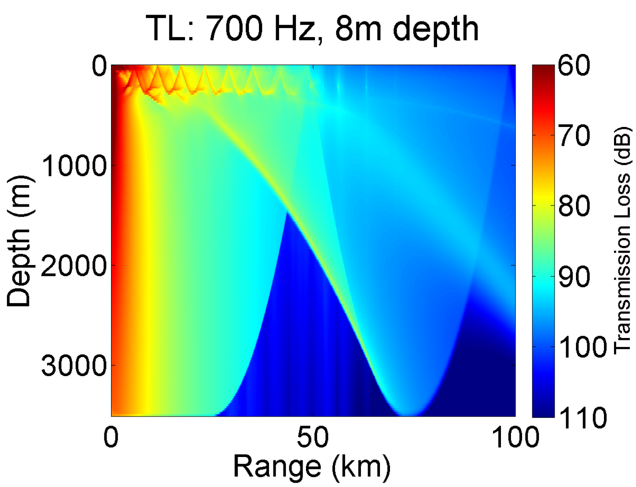

Figure 13 Transmission loss corresponding to the 2011 sound speed data. A loss-less surface reflection is assumed for simplicity.

The corresponding plot for 150 m is shown in Figure 14. Here the source is in the duct, and direct path propagation is visible out to the maximum range. If it were possible to position both the transmitter and receivers at this depth, then a direct path without the loss due to surface scatter could be available, though refracted and reflected energy would be present as well (for example as shown at close range in Figure 4). Additional work to analyze whether this duct is present through the seasons where the ice-based communications and navigation system would be deployed is necessary to see if the expense of the deeper source would be justified.

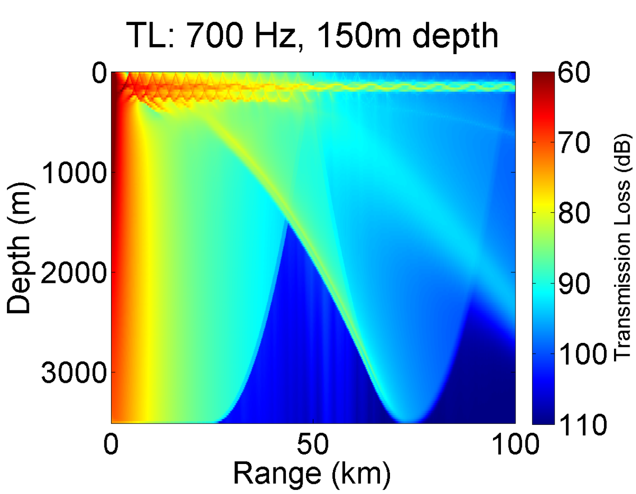

Figure 14 TL for a 150 m source showing the resulting ducted energy.

B. Experimental Setup

The experimental setup included four remote receivers, located 10, 20, 30 and 40 nmi (approximately 19, 37, 56, and 75 km) from the base camp, each with two hydrophones, one at 25 m depth, the other at 75 m. At the base camp the source was positioned at 8, 25, and 150 m depths. Not all combinations are discussed here. It will become evident that the propagation patterns described above will come into play in the SNR achieved for each combination.

C. Comparing Bandwidth

One of the experiments that was conducted entailed transmission of different bandwidth FM sweeps. Both 5 and 10 second signals were transmitted using bandwidths of 1.5 to 32 Hz centered at the same carrier. The sweeps were sent consecutively with sufficient time between each one to ensure the channel was clear. The results are shown in Figure 15, where the effect of additional bandwidth is clearly seen in the increased resolution of the arriving rays. The time span of the majority of the energy is approximately 1 second. The most striking thing to note is that the time of arrival estimate clearly improves with bandwidth, in particular from 1.5 to 4 Hz where the initial arrival group is first resolved. Absent the multipath, high SNR allows accurate time of arrival estimates on what look like very broad peaks, and lower bandwidth alone is not necessarily an impediment. However, in this case, the later energy skews the position of the peak and adds bias to the arrival estimate.

The result shown in Figure 15 demonstrates that short sweeps can provide very good SNR even at 75 km, and based on a closer look at the 32 Hz bandwidth result, may provide 50 m accuracy as opposed to order 750 m for the 1.5 Hz bandwidth case. An important next step in evaluating these results is determining the path that the first arrival traveled so that the travel time can be accurately converted to distance.

The other note of interest from Figure 15 is the total delay spread (in symbols) required for the equalizer feed-forward filters to span. For the 1 second spread, 12 symbols per second requires 24 T/2 spaced taps, etc. Signals to 96 sps were transmitted during the ICEX 2011 test, with 12 to 48 being the most successful at the farther stations. The 48 sps signal would require 96 taps to cover the multipath fully, but as the energy is concentrated in the first 200-300 msec, that many is not required. A sensitivity analysis to determine the optimal number of taps is another future area of work.

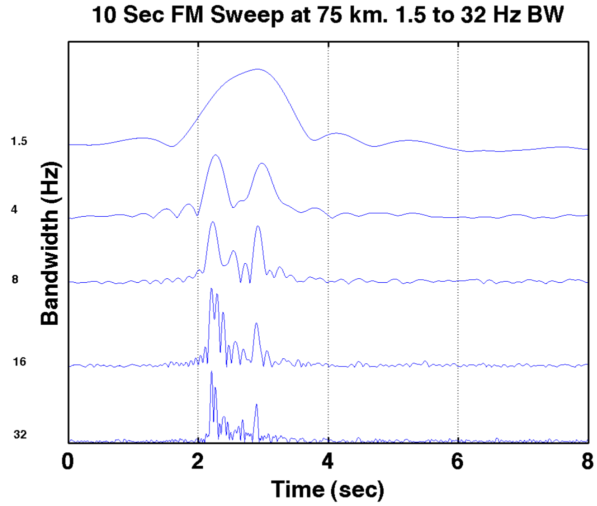

Figure 15 Matched-filter of sweeps of 1.5 to 32 Hz bandwidth (top to bottom) at the maximum range during the ICEX 2011 experiment.

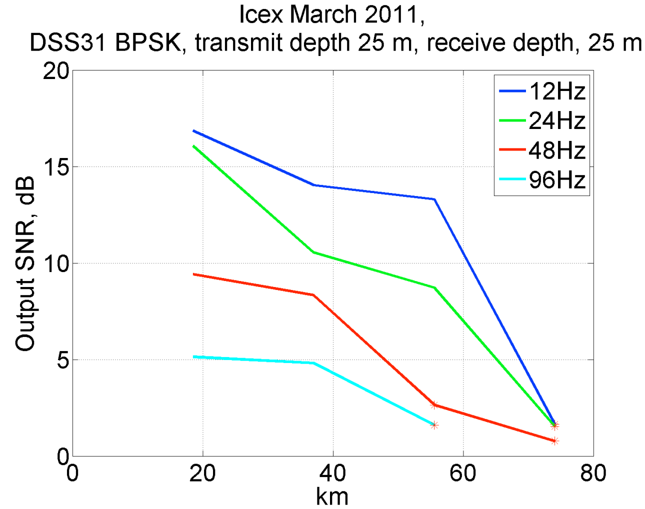

Figure 16 SNR at the output of the adaptive equalizer for the 25m-25m transmit-receiver depth case.

D. *Acoustic Communications*

The signal used for phase coherent communications was a QPSK signal with a spreading code of 31 chips followed by a rate 0.9 convolutional code. The symbols can be interpreted at the full rate (12, 24, 48 and 96 symbols per second), or by applying the spreading code and outer code. As discussed above for the Fram Strait results, the metric used to measure receiver performance is the SNR at the output of the equalizer, because it can be used to estimate the best feasible data rate. The implementation of the equalizer used here de-spreads the code within the inner loop and then uses the estimated transmitted symbols as decisions for feedback. This can be thought of as operating in training mode, but with delayed feedback of the equalizer taps of up to one spreading code length.

The results presented below are the average of three packets, and thus the potential variance is high. Limitations in the duration of the experiment limited the total amount of data that could be collected.

25m source, 25m receiver. In this case the SNR supports 12 and 24 Hz bandwidth out to 55 km, but it drops considerably at 75 km, and decoding is not successful at the maximum range (Figure 16).

25m source, 75m receiver. Here the results are considerably better than at 25 m depth. The output SNR for the 12 and 24 Hz cases is approximately 8 and 5 dB, respectively, high enough for symbol rate communications at 12 Hz, and just below that threshold at 24 Hz. The SNR was higher at closer range as well, highlighting the difference that source-receiver depth makes (Figure 17). The energy per bit for the 96 Hz bandwidth signal is simply too low for the long ranges without adding significant spreading or coding.

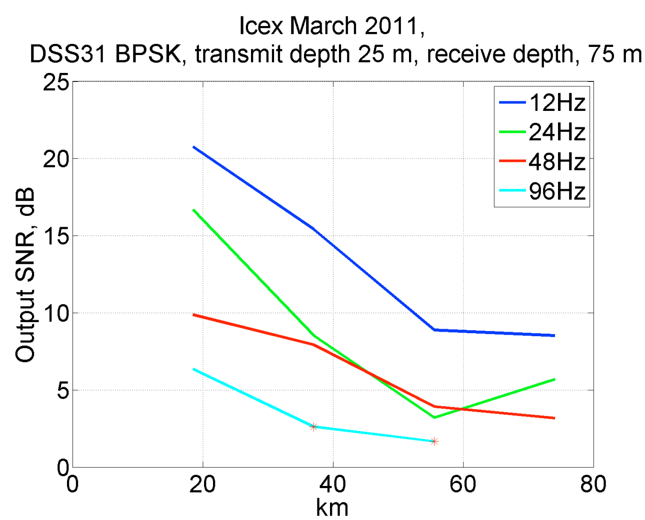

Figure 17 SNR at the output of the adaptive equalizer for the 25m-75m transmit-receiver depth case.

V. Conclusions

The results presented here are an initial step toward a communications and navigation capability for use under arctic ice. The communications aspect is particularly important for future systems where telemetry must be provided along with ranging, in order to inform receivers where the source is currently located as it drifts with the ice. A second important result was demonstrating that 700 and 900 Hz sources could provide both the bandwidth necessary for phase-coherent communication, and ranges to approximately 100 km. Previous work in tomography which proved that propagation under ice was feasible [3, 4], utilized swept-FM sources at 200-300 Hz, which are much larger and expensive, and do not allow phase-coherent modulation.

Some additional analysis of the data collected on these two experiments remains to be done. Of immediate interest is matching the received ray observations to models in order to identify their propagation paths. This will allow estimates of scattering loss for these particular channels to be made, important for extrapolating to longer ranges and also for calculating range from observed travel time. The 10 km spacing data from the Fram Strait will be used for that work.

In addition, a significant amount of FM sweep data was transmitted during the tests as a backup for the coherent communication. There will be a cross-over point where PSK will no longer be viable except with very long spreading sequences or codes, and at that point it may be more effective to use sweeps instead, despite the very low rate (on order 1 bit per 5 seconds). These trade-offs will be studied as part of the design for an integrated communication and navigation system for the ONR Marginal Ice Zone DRI project where gliders from APL-UW will use real-time location information to sample under the ice.

ACKNOWLEDGMENTS

Research in the arctic is inherently collaborative and support that includes infrastructure such as ice camps and ice breaking vessels is incredibly valuable. This work could not have been done without that non-financial support.

The WHOI Arctic Research Initiative provided financial support from 2008-2010 which allowed participation in the Norwegian Fram Strait experiment and the ICEX 2011 experiment. Hanne Sagen and the scientists and crew aboard the K/V Svalbard provided time and assistance during the 2010 Fram Strait cruise. The Arctic Submarine Laboratory and the Office of Naval Research supported logistics for participation in the 2011 ICEX north of Alaska. NPS provided CTD data from the 2009 and 2011 ICEX used in the transmission loss modeling presented here. Authoring and presenting this paper was supported by the ONR Marginal Ice Zone DRI, grant N00014-12-1-0176.

REFERENCES

1. C. Lee, J.G., *ANCHOR: Acoustic Navigation and Communication for High-latitude Ocean Research, Report from an International Workshop, University of Washington, 2006*, 2006.
2. Morozov, A., T. Altshuler, C. Jones, L. Freitag, P. Koski, and S. Singh, , *Underwater acoustic technologies for long-range navigation and communications in the Arctic*, in *Proceedings of the Undersea Acoustic Measurement Conference 2011 (UAM2011)*2011: Kos, Greece.
3. Jin, G., J. F. Lynch, R. Pawlowicz, and P. Wadhams, *Effects of sea ice cover on acoustic ray travel times, with applications to the Greenland Sea tomography experiment.* J. Acoust. Soc. Am., 1993. 94: p. 1044-1057.
4. Jin, G., J.F. Lynch, R. Pawlowicz, and P. Worcester, *Acoustic scattering losses in the Greenland Sea marginal ice zone during the 1988–89 tomography experiment.* J. Acoust. Soc. Am., 1994. 96: p. 3045-3053.
5. Sutton, P.J., P.F. Worcester, G. Masters, B.D. Cornuelle, and J. F. Lynch, *Ocean mixed layers and acoustic pulse propagation in the Greenland Sea.* J. Acoust. Soc. Am., , 1993. 94: p. 1517-1526.
6. Sagen, H., et. al., *The Fram Strait acoustic tomography system*, in *Proc. European Conference on Underwater Acoustics*2008: Paris, France.